Boson peak as a consequence of rigidity: A perturbation theory approach

Hugo M. Flores-Ruiz and Gerardo G. Naumis

Instituto de Física, Universidad Nacional Autónoma de México (UNAM), Apartado Postal 20-364, 01000, México, Distrito Federal, Mexico.

(Received 17 December 2010; revised manuscript received 2 March 2011; published 23 May 2011)

Some evidence is provided that the boson peak and floppy modes share a common origin. In the particular case of periodic systems, we show how a boson peak occurs as a consequence of a *reduction of constraints in an overconstrained lattice*, in contrast to floppy modes, which occur for a *reduction of constraints in a flexible or isostatic lattice*. In fact, the present approach allows us to follow the transformation of the boson peak into a floppy mode when a system goes from rigid to flexible. We use perturbation theory and Green's functions to see how resonances appear in the low-frequency region of the local vibrational density of states. For overconstrained lattices, we found that the boson peak frequency depends on the square root of the coordination of the lattice, and is at most 0.3 of the Debye frequency, a value close to the observed experimental ratio of 0.1. We also obtain the expected Rayleigh scattering for overconstrained networks, while we predict a different scattering for isostatic networks due to their critical nature. As an example, the effects of removing constraints are analyzed in a face-center-cubic lattice, and the same consequences are observed in a square network with and without diagonal links.

DOI: 10.1103/PhysRevB.83.184204 PACS number(s): 64.70.kj, 64.70.Q−, 61.43.Fs

I. INTRODUCTION

Our conceptual understanding of the microscopic nature of low-frequency vibrational modes (LFVMs) in glasses is not complete when compared with those in crystalline materials.[1,2] For example, the vibrational density of states (VDOS) in glasses displays an anomalous excess of LFVM.[3] Such modes are important not only for the related physical properties, like specific heat, heat conduction, etc., but also for the poorly understood process of glass transition.[4–6]

In fact, it is possible to estimate the glass transition temperature, fragility, entropy, etc., by using such modes.[7–9] Thus, the understanding of LFVMs is a subject of paramount importance. However, in the literature usually two kinds of anomalies are recognized in glasses. One is the excess of states due to floppy modes.[10,11] This type arises from a low coordination of the atomic network,[12–15] and has been successfully explained by the rigidity theory (RT) proposed by Phillips and Thorpe.[10,11] In essence, it says that each covalent bond can be treated as a mechanical constraint.[10] As a result, one can classify the rigidity properties into three classes: overconstrained, isostatic, and floppy, depending on the number of constraints and available degrees of freedom.[11] If the number of constraints is less than the dimensionality of the configurational space, then there is a fraction of modes that have nearly zero frequency and the system is flexible. Let us be more precise, if a system has N atoms, then there are DN degrees of freedom, where D is the space dimensionality. Suppose that there are N_c constrictions due to bonding, and $D(D+1)/2$ trivial modes (translations and rotations). The difference between them, $N_f = DN - N_c - D(D+1)/2$, is the number of floppy modes. When $N_f = 0$ such a system is *isostatic* and has the minimal number of constraints required to make the system rigid. When $N_c > DN$, the system is overconstrained and thus rigid. Many physical properties of glasses are dependent on such rigidity classification, including a self-organized stress-free intermediate phase.[16–19] The other important kind of low-frequency anomaly is a feature dubbed the "boson peak".[3] At low frequencies in crystals, the VDOS goes like $g(\omega) \propto \omega^{D-1}$, where ω is the frequency. The VDOS normalized by ω^{D-1} is a quantity $g(\omega)/\omega^{D-1}$ called the reduced vibrational density of states (RVDOS). The boson peak is a broad maximum in the RVDOS observed in glasses. The origin of the boson peak is not totally clear. For instance, some people claim that it is due to vibrations of clusters of atoms at typical sizes;[20,21] Elliot[22] suggests that it may arise from phonon scattering caused by density fluctuations at the medium length scale. Others say that such a peak is a consequence of the interaction between quasi-localized harmonic modes in glasses,[23] controlled by anharmonicity. Furthermore, it has been said through an assumption of randomly fluctuating transverse elastic constant, that the boson peak can emerge as a result of frozen disorder.[24] More recently, there have been arguments that, in fact, the boson peak is essentially due to the same mechanism that works for floppy modes, i.e., a weak connectivity of the solid.[26] A strong support for this point of view is that some crystals, like SiO_2, present a boson peak.[25,26] This means that disorder is not an essential feature to sustain a boson peak.[25] Concerning this point, in a previous recent work we showed,[27] using molecular dynamics, that, for Lennard–Jones binary glass, the boson peak is related to the rigidity properties. During the simulations it was observed that, in fact, it was possible to produce a similar peak in a face-center-cubic (FCC) lattice.[27] This led us to the possibility of finding the analytic relationship between rigidity and low-frequency anomalies by modifying periodic systems, as has been done for the elastic constants.[28,29]

The aim of this paper is to study, by using perturbation theory and Green's functions, the consequences on the LFVM of a progressive weakening connectivity in a lattice, done by cutting bonds on a overconstrained or isostatic network. As a starting point, we will consider two- and three- dimensional lattices. Notice that such a study was made by Thorpe and co-workers[28] many years ago. However, in such works the main focus was the scaling of the elastic modulus in the transition for the rigid to flexible lattice. Here we will concentrate our efforts in the effect on the VDOS of reducing *the connectivity*

of a rigid lattice. As we will see, resonances arise in the local vibrational density of states (LVDOS) in the low-frequency region, with a scattering proportional to q^4 (where q is the wave vector inversely proportional to the mean free path, as happens in the boson peak), which is known as a kind of Rayleigh scattering.[30] In that sense, the present work indicates that the boson peak is mainly composed of quasi-local vibrations.[31] However, here we will give evidence that the boson peak occurs as a consequence of a weakening connectivity in a rigid lattice, which is akin to how floppy modes occur for a weakening connectivity when a system is already flexible. This work is organized as follows, in Sec. II we present the analytical results of cutting bonds in rigid lattices. In Sec. III, we show the numerical results of the same process, including a FCC, a two-dimensional network with diagonal bond and a linear chain. The latter is a representative example of an isostatic system. Finally, the conclusions are given in Sec. IV the conclusions are given.

II. CUTTING BONDS IN RIGID LATTICES

To see the consequences of reducing the connectivity on the LVDOS of a rigid lattice, here we will consider disorder by cutting bonds in periodic systems. We start with the most simple idea: to cut a link between two particles and then check what occurs in the LVDOS/ω^2 by using perturbation theory. Then we will generalize the results for a weak concentration of diluted bonds. It is worthwhile mentioning that this perturbation approach is exact if only one bond is broken. The result is valid in any lattice or dimension, since all terms (or diagrams) of the series can be summed. For a finite concentration of broken bonds, the following approach is a good approximation for low concentrations of broken bonds, say less than 5%. However, for a higher concentration of disorder, the perturbation approach can be used considering some modifications that are essentially similar,[28] as we discuss below. In a real system, the rigidity of the nonperturbed system can be determined from the average coordination number and some elastic properties.[16] Broken bonds are obtained by radiation damage, thermal processes, or chemical doping. Consider a rigid lattice with an harmonic Hamiltonian $\mathbf{H_0}$. If few bonds are changed on this network, the new Hamiltonian $\mathbf{H}$ can be written as,[32]

$$\mathbf{H} = \mathbf{H_0} + \mathbf{V},$$

where the matrix $\mathbf{V}$ contains the changes made. The well known Green's functions formalism and perturbation theory can be used to obtain the new frequency spectrum.[34] The Green's function $\mathbf{G}$ is defined as,

$$G_{\nu\beta}(l,j) = \lim_{\eta\to 0} \frac{1}{M} \sum_{\mathbf{q}} \frac{\chi^*_{\nu,\mathbf{q}}(l)\chi_{\beta,\mathbf{q}}(j)}{\omega^2 + i\eta - \omega^2(\mathbf{q})}, \tag{1}$$

where the sum is carried over the eigenvectors $\mathbf{q}$ with eigenvalues $\omega^2(\mathbf{q})$ of $\mathbf{H}$. M is the particle mass, and $\chi_{\beta,\mathbf{q}}(j)$ is the β component of the eigenmode $\mathbf{q}$ displacement at site j. $\mathbf{G}$ can be written in terms of the unperturbed Green's function $\mathbf{G}_0$ of $\mathbf{H}_0$ as follows:[34]

$$\mathbf{G} = \frac{\mathbf{G}_0}{\mathbf{I} - \mathbf{V}\mathbf{G}_0} = \mathbf{G}_0 + \mathbf{G}_0\mathbf{T}\mathbf{G}_0, \tag{2}$$

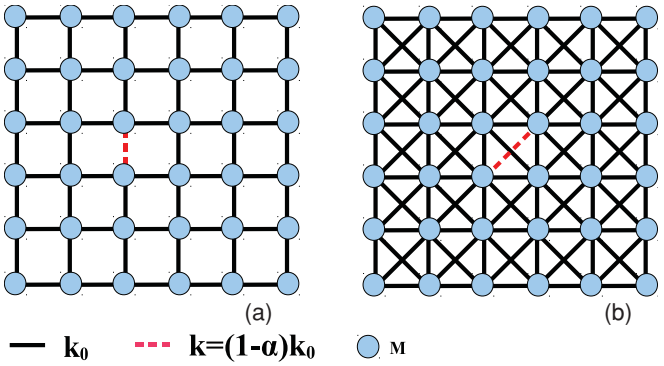

FIG. 1. (Color online) Examples of two kinds of rigid lattices; (a) isostatic (using cyclic boundary conditions), and (b) overconstrained. The diluted bond constraint $k \equiv k_0 - \alpha k_0$ is also shown. When $\alpha = 1$, the bond is removed. M is the particles' mass.

where $\mathbf{I}$ and $\mathbf{T} = \mathbf{V}(\mathbf{I} - \mathbf{V}\mathbf{G}_0)^{-1}$ are the identity and scattering matrices respectively. Equation (2), is rewritten as

$$\mathbf{G} = \frac{\mathbf{G}_0 \mathrm{adj}(\mathbf{I} - \mathbf{V}\mathbf{G}_0)}{\det(\mathbf{I} - \mathbf{V}\mathbf{G}_0)}. \tag{3}$$

The total VDOS ($\rho(\omega)$) of the whole system $\mathbf{G}$ is

$$\rho(\omega) = 2\omega\rho(\omega^2) = -\frac{2\omega}{\pi}\mathrm{Im}\{\mathrm{Tr}\mathbf{G}\}. \tag{4}$$

As was mentioned before, we are interested in a diluted bond. In this case, two sites are involved. Then we just keep a $2D \times 2D$ matrix $\mathbb{V}$ of the whole $\mathbf{V}$. $\mathbb{V}$ can be written as[32]

$$\mathbb{V} = \begin{pmatrix} \Delta(1,1) & \Delta(1,2) \\ \Delta(2,1) & \Delta(2,2) \end{pmatrix}. \tag{5}$$

In essence, Δ is related to the spring's constant (in the harmonic approach) on sites 1 and 2. Following this idea, we take a small $2D \times 2D$ matrix $\mathbb{G}_0$ of the whole matrix $\mathbf{G}_0$,

$$\mathbb{G}_0 = \begin{pmatrix} G_0(1,1) & G_0(1,2) \\ G_0(2,1) & G_0(2,2) \end{pmatrix}. \tag{6}$$

Here $G_0(1,1)$ refers to the Green's function on site 1 (which is a $D \times D$ matrix), $G_0(2,2)$ on site 2, and $G_0(1,2)$ or $G_0(2,1)$ are related with the interaction between them. In fact, $G_0(1,1) = G_0(2,2)$ and $G_0(1,2) = G_0(2,1)$.[32,33] It follows that in such a reduced scheme, $\mathbb{G} = \mathbb{G}_0 + \mathbb{G}_0\mathbb{T}\mathbb{G}_0$ and the scattering matrix is $\mathbb{T} = \mathbb{V}(1 - \mathbb{V}\mathbb{G}_0)^{-1}$.

To show in an explicit way how perturbation theory works when a bond is cut, we define the link perturbation as $k \equiv k_0 - \alpha k_0$. α is a dimensionless parameter between 0 and 1. $\alpha = 0$ means that the bond is nonperturbed, while for $\alpha = 1$, the bond between sites 1 and 2 is removed. This fact is explained in Fig. 1, where we show how a bond is diluted in over-constrained and isostatic lattices. Under that consideration, define[28] $\Delta(l,j) = (k - k_0)\widehat{r_{12}}\widehat{r_{12}}m_{lj}$, where $\widehat{r_{12}}$ is the vector in the direction of the vector that joins site 1 with 2, and $m_{lj} = \delta_{1l}\delta_{1j} + \delta_{2l}\delta_{2j} - \delta_{1l}\delta_{2j} - \delta_{2l}\delta_{1j}$.

It is possible to show that the scattering matrix is given by[28]

$$\mathbb{T}(l,j) = \frac{-\alpha k_0}{[1 + 2\alpha k_0 \widehat{r_{12}} \cdot (G_0(1,1) - G_0(1,2)) \cdot \widehat{r_{12}})]} \widehat{r_{12}}\widehat{r_{12}}m_{lj}. \tag{7}$$

The denominator, which eventually leads to resonant states, can be simplified using the following trick. The pure system Green's function follows the equation of motion,

$$M\omega^2 G_0(1) = 1 + \frac{Z}{D} k_0 \widehat{r_{12}} \cdot (G_0(1,1) - G_0(1,2)) \cdot \widehat{r_{12}}, \quad (8)$$

where $G_0(1)$ is the magnitude of the isotropic site's diagonal Green's function $G_0(1,1)$ and Z is the coordination of the lattice. Inserting Eq. (8) into Eq. (7), we get,

$$\mathbb{T}(l,j) = \frac{-\alpha k_0}{\left[1 + \frac{2\alpha D}{Z}(M\omega^2 G_0(1) - 1)\right]} \widehat{r_{12}}\widehat{r_{12}} m_{lj}. \quad (9)$$

The resulting LVDOS at sites 1 and 2 ($\rho_d(\omega)$) is calculated from[34]

$$\rho_d(\omega;\alpha) = 2\omega\rho_d(\omega^2;\alpha) = -\frac{2\omega}{\pi}\mathrm{Im}\{\mathrm{Tr}\mathbb{G}\}. \quad (10)$$

The resonance condition is obtained when the denominator in Eq. (7) is nearly zero, which allows us to find the frequency of the resonant peak (ω_R) as a solution of

$$1 + \frac{2\alpha D}{Z}(M\omega^2 \mathrm{Re}G_0(1) - 1) \approx 0, \quad (11)$$

$$\frac{2\alpha D}{Z} M\omega^2 \mathrm{Im}G_0(1) \approx 0. \quad (12)$$

The equation concerning the real part locates the resonance, while the other determines the decay time. Since $\mathrm{Im}G_0(1) \sim -\pi\rho(\omega^2)/M$, the unperturbed density of states at such resonant frequency needs to be small, a condition that holds in the lower part of the vibrational spectrum. Such a condition is akin to the one obtained for an impurity mass.[35]

From the previous equation, we can also obtain the transition probability per unit time of the state $\mathbf{q}_i$ to $\mathbf{q}_f$, $W_{\mathbf{q}_i\mathbf{q}_f} = |\langle \mathbf{q}_f|\mathbb{T}(1,1)|\mathbf{q}_i\rangle|^2 \delta(M\omega_i^2 - M\omega_f^2)$. For states that follow the resonance condition, Eq. (11), $|\langle \mathbf{q}_f|\mathbb{T}(1,1)|\mathbf{q}_i\rangle|^2$ can be written as

$$|\langle \mathbf{q}_f|\mathbb{T}(1,1)|\mathbf{q}_i\rangle|^2 = \frac{A^2}{\left(\omega^2 - \omega_R^2\right)^2 + \Gamma^2}, \quad (13)$$

where the resonance width Γ, related to the decay time, and A are given by

$$\Gamma = \left.\frac{\omega^2 \mathrm{Im}G_0(1)}{\frac{d}{d\omega^2}(\omega^2 \mathrm{Re}G_0(1))}\right|_{\omega^2=\omega_R^2},$$
$$A^{-1} = \left.\frac{2DM}{Zk_0}\frac{d}{d\omega^2}(\omega^2 \mathrm{Re}G_0(1))\right|_{\omega^2=\omega_R^2}. \quad (14)$$

Although all of the previous results are valid for only one diluted bond, the arguments are easily extended for low concentrations (n) of sites with diluted bonds. Since the probability of having pure diluted bonds through a distance r is $e^{(r/a)\ln n}$, where a is the lattice parameter, most of the diluted bonds are surrounded by undisturbed bonds. As a consequence, one can safely use the virtual crystal approximation[32] (VCA). Under such a approximation, the VDOS is simply a weighted combination of the LVDOS at the diluted ($\rho_d(\omega)$) and undiluted bond sites ($\rho_{ud}(\omega)$),

$$\rho(\omega) = (1-n)\rho_{ud}(\omega) + n\rho_d(\omega). \quad (15)$$

Thus, a local resonant state is able to produce a peak of spectral weight n. When n is increased, there is more interaction between diluted bonds, and the resonant peak splits into many levels. In such case, the coherent potential approximation (CPA) method[32] can be used as an excellent approximation. Now we can build the connection with RT, since from Eqs.(11) and (12) we can discuss the case of overconstrained and isostatic systems.

A. Overconstrained systems

The usual Goldstone acoustic modes are present and $\omega = c\,\|\mathbf{q}\|$, where c is the average speed of sound. Thus, in D dimensions $\rho(\omega) \sim D^2\omega^{D-1}/\omega_D^D$ and $\mathrm{Im}G_0(1) \approx -\pi D^2\omega^{D-2}/2M\omega_D^D$, where ω_D is the Debye frequency. From this result and using $D = 3$, we can obtain $\mathrm{Re}G_0(1)$ from the Kramers–Kröning relations,

$$\mathrm{Re}G_0(1) = \frac{3^2}{M\omega_D^3}\left[-\omega_D + \frac{\omega}{2}\ln\left(\frac{\omega_D+\omega}{\omega_D-\omega}\right)\right]. \quad (16)$$

Using $\mathrm{Re}G_0(1)$ in Eq. (11), the resonant frequency (ω_R) is located at

$$\omega_R \approx \frac{\omega_D}{3}\sqrt{\frac{Z}{6\alpha} - 1}, \quad (17)$$

and the width (Γ) is

$$\Gamma \approx \frac{27\omega_R^4}{\left[11 - \frac{Z}{3\alpha}\right]\sqrt{\frac{Z}{6\alpha} - 1}\omega_D^2}. \quad (18)$$

Notice that, for a maximal packing corresponding to a FCC lattice, $Z = 12$ and for $\alpha = 1$, $\omega_R \approx 0.3\omega_D$ and $\Gamma \approx \omega_D^2/21$. For smaller coordinated systems, the fraction ω_R/ω_D is smaller, and thus here we provided a maximal bound for the resonance. This very rough value is in such qualitative agreement with the experimental fact that usually the boson peak frequency (Ω_b) is given by[31] $\Omega_b \approx 0.1\omega_D$. A more detailed computation can be done, taking into account the different speeds of sounds for each branch and a lesser degree of approximation in the Green's function. Finally, to check if a resonant state appears, it is necessary to verify that at least several oscillations are performed during the decay time, i.e., the real part needs to be higher than the imaginary part. In this case, from Eq. (16) is clear that for $\omega \ll \omega_D$, the real part ω

$$\mathrm{Re}G_0(1) \approx \frac{9}{M}\left[-\frac{1}{\omega_D^2} + \frac{\omega^2}{\omega_D^4}\right], \quad (19)$$

while the imaginary part is

$$\mathrm{Im}G_0(1) \approx -9\pi\omega/2M\omega_D^3, \quad (20)$$

from which it follows that

$$\frac{\mathrm{Im}G_0(1)}{\mathrm{Re}G_0(1)} \approx \frac{\pi}{2}\left(\frac{\omega_R}{\omega_D}\right). \quad (21)$$

In the worst-case scenario, this ratio is around 0.47 and decreases with the coordination of the lattice, which indicates that the states are always resonant. It is worthwhile mentioning that, in the following section, we show how an exact calculation in FCC lattice, which corresponds to the worst-case scenario, presents clearly a resonant state.

Also, we can analyze the behavior of the relaxation time τ and mean free path l of the scattering at low frequencies due to the lack of constraints. The time can be written as,

$$\tau^{-1} = c\sigma n, \tag{22}$$

where c is the sound velocity, σ is the total scattering cross section and n is the number of scatters per molecular volume V. σ is proportional to the sum over initial ($\mathbf{q}_i$) and final states ($\mathbf{q}_f$) of the transition probability per unit time $W_{\mathbf{q}_i\mathbf{q}_f}$, divided by the flux $j = c/V$ of the incoming particles.[34] Since we are dealing with elastic collisions, the sum over initial and final states is replaced by the density of initial and final states[37,38] $\sigma = V|\langle\mathbf{q}_f|\mathbb{T}(1,1)|\mathbf{q}_i\rangle|^2\rho_i(\omega)\rho_f(\omega)c^{-1}$.

At low frequencies and far from the resonance, Eq. (13) gives $|\langle\mathbf{q}_f|\mathbb{T}(1,1)|\mathbf{q}_i\rangle|^2 \approx A^2/\omega_R^2$. Using a Debye density of states as well as the concentration of scatter centers, the relaxation time is written as

$$\tau^{-1} \approx nV\frac{D^4A^2}{\omega_R^2\omega_D^{2D}}\omega^{2(D-1)}. \tag{23}$$

In three dimensions, τ^{-1} follows an ω^4 Rayleigh type of scattering, a feature that is well known to be associated with the boson peak.[30] Notice that here n is given by the number of diluted bonds, which turns out to be given by the change in the average coordination of the system ($\delta\langle Z\rangle$). The fragility of the system is related to[15] $\langle Z\rangle$, and thus here we provide a link between mean free path and fragility.

B. Isostatic systems

This is a delicate and interesting case, which appears in hyperstatic networks (linear, square, and cubic lattices). From constraint theory, is clear that if we cut a bond, a floppy mode appears.[26] However, it is instructive to learn how such mode is viewed from perturbation theory. In fact, the linear, square and cubic lattices, all have the same dispersion relationship for phonons, since the springs have projections only in perpendicular directions between themselves,[29] as can be seen in Fig. 1(a). Thus, for small ω, $\rho(\omega) \sim \omega^0$ as happens in general for other isostatic networks[26] (although it is worthwhile mentioning that for disordered isostatic systems, the Green's function displays very interesting properties due to multiplicative random processes).[36]

Let us work this case with more detail. Using the Green's function for a linear chain inside the spectrum, we have[34]

$$\mathrm{Im}G_0(1) \approx \frac{-2}{M\omega_m^2(1-x^2)^{1/2}}, \mathrm{Re}G_0(1) = 0, \tag{24}$$

where

$$x = 2(\omega/\omega_m)^2 - 1, \tag{25}$$

ω_m is the band edge, and

$$\begin{aligned}\mathrm{Im}G_0(1,2) &= \cos\phi(\omega)\mathrm{Im}G_0(1),\\ \mathrm{Re}G_0(1,2) &= -\sin\phi(\omega)\mathrm{Im}G_0(1),\end{aligned} \tag{26}$$

with the phase angle $\phi(\omega)$ defined as

$$\phi(\omega) = \tan^{-1}\left[\frac{\sqrt{1-x^2}}{-x}\right]. \tag{27}$$

The conditions for resonance, given by the poles of Eq. (9), are now written as

$$\mathrm{Im}(G_0(1) - G_0(1,2)) = [1-\cos\phi(\omega)]\mathrm{Im}G_0(1) \approx 0,$$
$$\mathrm{Im}G_0(1) \approx -[\alpha 2k_0\sin\phi(\omega)]^{-1}.$$

Also, from Eq. (24), it is easy to see that $\mathrm{Im}G_0(1) = -[2k_0\sin\phi(\omega)]^{-1}$. Thus, only for $\alpha = 1$, one of the conditions for resonance is satisfied and in fact, it holds for *all frequencies*. However, $[1-\cos\phi(\omega)]\mathrm{Im}G_0(1)$ is zero only at zero frequency, while it is nearly zero at low frequencies. Thus, the effect of cutting a bond is a tendency to smooth the whole LVDOS, as it will be corroborated numerically in the next section. The floppy mode appears at zero frequency as a resonance, but there is an additional softening of the spectrum at all frequencies. In fact, the nature of the mode is simple to understand. If one cuts a linear chain, the resulting lattice is made by two chains with free boundary conditions. Instead of having one center-of-mass mode, two center-of-mass modes appear, one for each piece of chain. Clearly, such a new mode cannot be the result of a localized mode due to the extended nature of the state. The softening of the LVDOS at the broken bond is just the vibrational spectrum at the free end.

As in the overconstrained case, we are interested in the scaling of τ^{-1}. We take Eq. (23), but in the present case $\rho(\omega) \sim \omega^0$; thus in the isostatic case the relaxation time due to scattering is

$$\tau^{-1} \sim \text{constant}. \tag{28}$$

We can say that isostatic systems present a uniform scattering throughout the spectrum, a feature that is anomalous when compared with overconstrained systems, but that is akin to the phenomena of critical opalescence. In that sense, this seems to be an exciting prediction concerning the critical nature of isostatic networks.[36]

III. SOME EXAMPLES OF CUTTING BONDS IN RIGID LATTICES

In this section, we give some examples that show how a resonance similar to the boson peak arises when we cut bonds in overconstrained networks and as well as in isostatic systems.

A. Overconstrained network: A FCC

We start by looking at the consequences of cutting bonds in a FCC structure. To achieve this goal, we diagonalize numerically the corresponding 3×3 dynamical matrix ($\mathbb{D}$). Its components can be written as (in units where the lattice parameter a is equal to one),

$$\begin{aligned}\mathbb{D}_{xx} &= 4k_0[2-\cos(q_x/2)\cos(q_z/2)-\cos(q_x/2)\cos(q_y/2)],\\ \mathbb{D}_{yy} &= 4k_0[2-\cos(q_x/2)\cos(q_y/2)-\cos(q_y/2)\cos(q_z/2)],\\ \mathbb{D}_{zz} &= 4k_0[2-\cos(q_x/2)\cos(q_z/2)-\cos(q_y/2)\cos(q_z/2)],\\ \mathbb{D}_{xy} &= \mathbb{D}_{yx} = 4k_0\sin(q_x/2)\sin(q_y/2),\\ \mathbb{D}_{xz} &= \mathbb{D}_{zx} = 4k_0\sin(q_x/2)\sin(q_z/2),\\ \mathbb{D}_{yz} &= \mathbb{D}_{yx} = 4k_0\sin(q_y/2)\sin(q_z/2).\end{aligned}$$

Then we take points (q_x,q_y,q_z) from the first Brillouin zone to diagonalize $\mathbb{D}$, and we use Eq. (1) with the corresponding

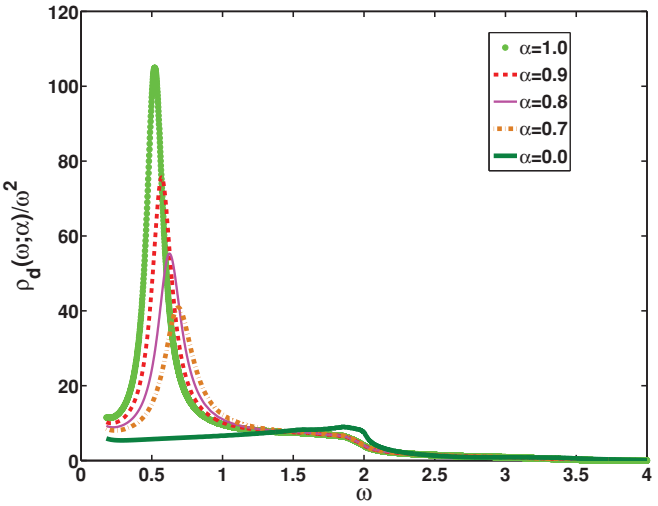

FIG. 2. (Color online) Evolution of the reduced vibrational density of sates $[\rho_d(\omega;\alpha)/\omega^2]$ with respect to the perfect FCC ($\alpha = 0$). When a bond is cut, $\alpha = 1$(circles, green on line), a peak arises in $\rho_d(\omega;\alpha = 1)/\omega^2$ on a minimal frequency.

eigenvectors and eigenfrequencies. In this way, we are able to obtain $\rho_d(\omega;\alpha)/\omega^2$ and the resonance condition, Eq. (11), which can be written for this case as

$$\mathrm{Re}G_0(1) \approx \left(1 - \frac{2}{\alpha}\right)\frac{1}{\omega^2}. \tag{29}$$

Figure 2 shows the evolution of $\rho_d(\omega\ ;\alpha)/\omega^2$ as a function of frequency. We see a peak at the lowest frequency when the bond is cut ($\alpha = 1$) in contrast to the perfect FCC lattice ($\alpha = 0$). We notice that ω_R decreases as $\alpha \longrightarrow 1$, producing a peak near the expected position. In Fig. 3, the real and imaginary parts of $G_0(1)$ are shown, as well as the resonance condition, Eq. (29), versus frequency.

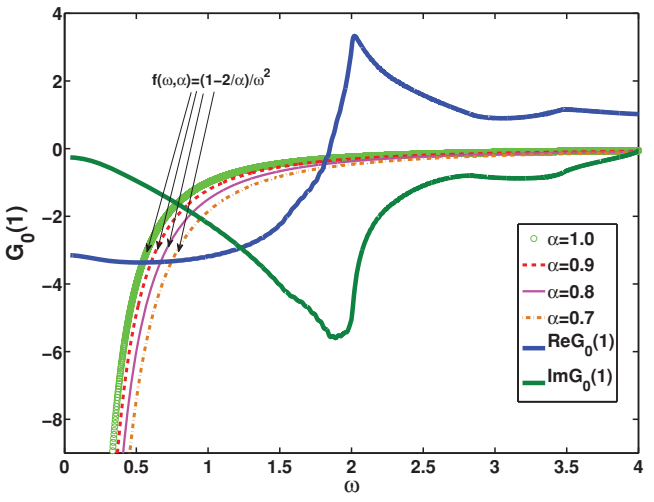

FIG. 3. (Color online) Real and Imaginary parts of $G_0(1)$ (blue and green lines, respectively) for the FCC lattice, and the function $f(\omega;\alpha) = [1 - 2/\alpha]/\omega^2$. The resonant frequencies (ω_R) are found at the intersection of the curves $\mathrm{Re}G_0(1)$ and $f(\omega;\alpha)$, over different alpha values. Notice how $\mathrm{Im}G_0$ goes to zero as the frequency is reduced.

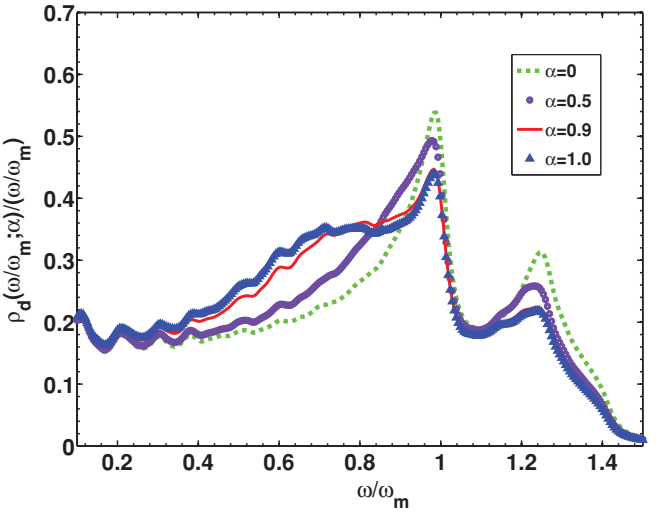

FIG. 4. (Color online) RVDOS $[\rho_d(\omega/\omega_m;\alpha)/(\omega/\omega_m)]$ for a square lattice with crossed diagonals. The case $\alpha = 0$ corresponds to the pure network, and then gradually a bond is removed up to $\alpha = 1$.

B. Overconstrained network: square lattice with diagonals

Now we want to test the same ideas in a different rigid network: a square lattice with diagonal bonds, as seen in Fig. 1(b). This time we do not have the Green's functions explicitly, but we can diagonalize the Hamiltonian. In this way, the eigenvalues are used to calculate $\rho_d(\omega/\omega_m;\alpha)$, using a network with $N = 1600$ sites, where ω_m is the spectrum edge frequency. In Fig. 4, we present the corresponding $\rho_d(\omega/\omega_m;\alpha)/(\omega/\omega_m)$. Here a resonance arises inside the band as a bond is diluted. As α goes from 1 to 0, we can observe how an excess of modes is built for low frequencies. Notice that the small oscillations near zero frequency are due to finite-size effects.

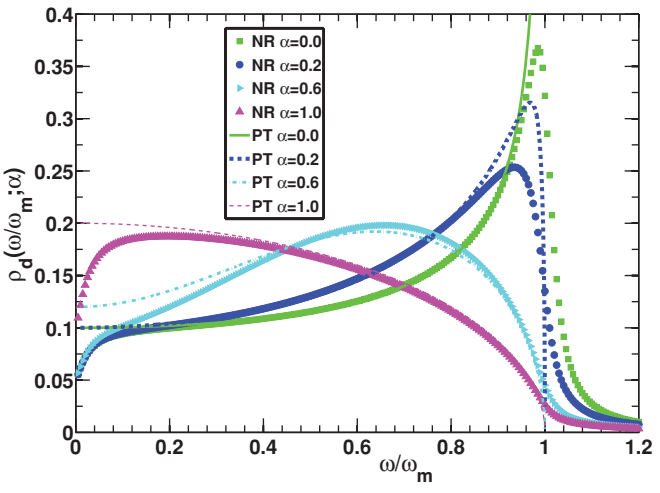

FIG. 5. (Color online) RVDOS $[\rho_d(\omega/\omega_m;\alpha)]$ of a large chain versus the normalized frequency for different α values of a diluted bond. The points and lines represent the numerical and theoretical results from perturbation theory, denoted by NR and PT, respectively. We can see an increase of low, frequency modes and a smoothing of the spectrum. The differences between PT and NR at very low frequencies are due to finite size effects.

C. Isostatic networks: Linear, square, and cubic lattices

Finally, to see what happens when a link is cut in isostatic systems, we study a linear chain with periodic boundary conditions. Actually, this chain is equivalent to the square and cubic lattices[29] with periodic boundary conditions. The case of the isostatic square lattice is shown in Fig. 1(a), from where it is easy to figure out why the dispersion relationship is the same as in the linear chain case. It is worthwhile mentioning that the periodic boundary conditions are crucial, since if a chain has N sites, N bonds are required to have as many constraints as degrees of freedom. Such periodic isostatic lattices are known as hyperstatic. The analysis of this linear lattice is made by using the Green's functions at sites[34] h and l;

$$G_0(h,l) = \frac{1}{2k_0 i\sqrt{1-x^2}}[-x + i\sqrt{1-x^2}]^{|h-l|}, \tag{30}$$

where $x = 2(\omega/\omega_m)^2 - 1$ and $\omega_m^2 = 4k_0/M$ is the maximum frequency. As in the previous cases, we are interested in a bond perturbation between sites 1 and 2. From Eq. (30),

$$G_0(1,1) = \frac{-i}{2k_0\sqrt{1-x^2}}, \quad G_0(1,2) = -xG_0(1,1) + \frac{1}{2k_0}. \tag{31}$$

Using Eqs. (31) and (10), we obtain the LVDOS at sites 1 and 2 $\rho_d(\omega)$ as

$$\rho_d(\omega/\omega_m;\alpha) = \frac{-2\omega/\omega_m \mathrm{Im}G_0(1,1)}{\pi} \frac{\left[\left(1-\alpha+2\alpha\left(\frac{\omega}{\omega_m}\right)^2\right)(1-\alpha) + 4\alpha^2(2k_0\mathrm{Im}G_0(1,1))^2\left(\frac{\omega}{\omega_m}\right)^4\left(1-\left(\frac{\omega}{\omega_m}\right)^2\right)\right]}{[1-\alpha]^2 + \left[2\alpha\left(\frac{\omega}{\omega_m}\right)^2(2k_0\mathrm{Im}G_0(1,1))\right]^2}. \tag{32}$$

When $\alpha = 0$, we have the unperturbed $\rho(\omega)$ as

$$\rho(\omega/\omega_m;\alpha = 0) = \frac{-2}{\pi}\frac{\omega}{\omega_m}\mathrm{Im}G_0(1,1), \tag{33}$$

and when the bond is totally removed, $\alpha = 1$, the LVDOS is written as,

$$\rho_d(\omega/\omega_m;\alpha = 1) = 2\left(1 - \left(\frac{\omega}{\omega_m}\right)^2\right)\rho(\omega/\omega_m;\alpha = 0). \tag{34}$$

In Fig. 5, the behavior of Eqs. (33) and (34) is displayed for such isostatic systems. These equations are compared with the numerical calculation in a chain with $N = 1000$ sites. The frequencies are obtained when the dynamical matrix is diagonalized. The agreement between the formal solution and the numerical result is excellent, except at very low frequencies, where there is a small difference due to finite-size effects. We can see an increase in $\rho_d(\omega/\omega_m;\alpha = 1)$ at $\omega = 0$ and a tendency to smooth the spectrum. This feature could be interpreted as a resonance at $\omega = 0$ but with a large width.

IV. CONCLUSIONS

We have made an analogy between the boson peak and the resonances that emerge when bonds are cut in rigid lattices. As an example, the cases of the FCC and the square lattice with diagonal bonds are worked in detail. A similar analysis is made on isostatic structures. We gave some evidence that the boson peak arises as an extension of the concept of floppy modes but for overconstrained networks, i.e., if the number of constraints is reduced in an overconstrained system, a boson peak appears at a finite frequency, while in a flexible system, the reduction leads to a peak at zero frequency. The ratio between the Debye frequency and the boson peak position is given by $\omega_R/\omega_D \approx \sqrt{(Z/6)-1}/3$, where Z is the coordination of the network. This produces a bound around 0.3 for high coordination lattices, which is well compared with the empirical observation that gives 0.1. In the case of hyperstatic networks, we have shown how the process of appearance of a floppy mode can be seen as a resonance at zero frequency, while the spectrum is very sensitive to perturbations. The usual Rayleigh scattering was found for the boson peak, while a kind of critical scattering could occur in isostatic networks.

ACKNOWLEDGMENTS

We thank DGAPA-UNAM projects IN-100310-3 and CONACyT 48783-F, 50368. The calculations were performed on Kanbalam and Bakliz supercomputers at DGSCA-UNAM.

[1] J. Langer, Phys. Today **60**(2), 8 (2007).
[2] P. K. Gupta and J. K. Mauro, J. Chem. Phys. **130**, 094503 (2009).
[3] M. I. Klinger, Phys. Rep. **492**, 111 (2010).
[4] A. Huerta and G. G. Naumis, Phys. Rev. Lett. **90**, 145701 (2003).
[5] G. G. Naumis and H. M. Flores-Ruiz, Phys. Rev. B **78**, 094203 (2008).
[6] H. M. Flores-Ruiz and G. G. Naumis, J. Chem. Phys. **131**, 154501 (2009).
[7] G. G. Naumis, Phys. Rev. B **73**, 172202 (2006).
[8] G. G. Naumis, J. Non-Cryst. Solids **352**, 4685 (2006).
[9] G. G. Naumis, Phys. Rev. B **61**, R9205 (2000).
[10] J. C. Phillips, J. Non-Cryst. Solids **34**, 153 (1979).
[11] M. F. Thorpe, J. Non-Cryst. Solids **57**, 355 (1983).
[12] K. Trachenko, M. T. Dove, V. Brazhkin, and F. S. El'kin, Phys. Rev. Lett. **93**, 135502 (2004).
[13] I. P. Swainson and M. T. Dove, Phys. Rev. Lett. **71**, 193 (1993).
[14] M. T. Dove, M. J. Harris, A. C. Hannon, J. M. Parker, I. P. Swainson, and M. Gambhir, Phys. Rev. Lett. **78**, 1070 (1997).

[15]W. A. Kamitakahara, R. L. Cappelletti, P. Boolchand, B. Halfpap, F. Gompf, D. A. Neumann, and H. Mutka, Phys. Rev. B **44**, 94 (1991).
[16]D. Selvanathan, W. J. Bresser, and P. Boolchand, Phys. Rev. B **61**, 15061 (2000).
[17]Y. Wang, J. Wells, D. G. Georgiev, P. Boolchand, K. Jackson, and M. Micoulaut, Phys. Rev. Lett. **87**, 185503 (2001).
[18]D. Novita, P. Boolchand, M. Malki, and M. Micoulaut, Phys. Rev. Lett. **98**, 195501 (2007).
[19]A. Huerta and G. G. Naumis, Phys. Rev. B **66**, 184204 (2002).
[20]V. K. Malinovsky, V. N. Novikov, and A. P. Sokolov, Phys. Lett. A **153**, 63 (1991).
[21]T. Pang, Phys. Rev. B **45**, 2490 (1992).
[22]S. R. Elliot, Europhys. Lett. **19**, 201 (1992).
[23]V. L. Gurevich, D. A. Parshin, and H. R. Schober, Phys. Rev. B **67**, 094203 (2003).
[24]W. Schirmacher, Europhys. Lett. **73** (2006).
[25]M. Wyart, Ann. Phys. Fr. **30**, 1 (2005).
[26]M. Wyart, L. E. Silbert, S. R. Nagel, and T. A. Witten, Phys. Rev. E **72**, 051306 (2005).
[27]H. Flores-Ruiz, G. G. Naumis, and J. C. Phillips, Phys. Rev. B **82**, 214201 (2010).
[28]S. Feng, M. F. Thorpe, and E. Garboczi, Phys. Rev. B **31**, 276 (1985).
[29]A. Souslov, A. J. Liu, and T. C. Lubensky, Phys. Rev. Lett. **103**, 205503 (2009).
[30]J. E. Graebner, B. Golding, and L. C. Allen, Phys. Rev. B **34**, 5696 (1986).
[31]B. Ruffle, D. A. Parshin, E. Courtens, and R. Vacher, Phys. Rev. Lett. **100**, 015501 (2008).
[32]R. J. Elliot, J. A. Krumhansl, and P. L. Leath, Rev. Mod. Phys. **46**, 465 (1974).
[33]T. Morita, and T. Horiguchi, J. Phys. Soc. Jpn. **30**, 957 (1971).
[34]E. N. Economou, *Green's Functions in Quantum Physics*, 3rd. ed. (Springer, Berlin, 2006).
[35]P. G. Klemens, Solid State Phys. **7**, 1 (1958).
[36]C. Moukarzel, J. Phys. Condens. Matter **14**, 2379 (2002).
[37]C. T. Walker and R. O. Pohl, Phys. Rev. **131**, 1433 (1963).
[38]P. G. Klemens, Proc. R. Soc. London Sec. A **208**, 108 (1951).